Thermal Decomposition Mechanisms of Methanol, Ethanol, and 1-Propanol on the Si (100)-2× 1 Surface

ARTICLE *in* THE JOURNAL OF PHYSICAL CHEMISTRY C · MAY 2008

Impact Factor: 4.77 · DOI: 10.1021/jp711840f

2 AUTHORS, INCLUDING:

Cheol Ho Choi
Kyungpook National University
111 PUBLICATIONS **2,117** CITATIONS

SEE PROFILE

Thermal Decomposition Mechanisms of Methanol, Ethanol, and 1-Propanol on the Si(100)-2 × 1 Surface

Jieun Cho and Cheol Ho Choi*

Department of Chemistry, College of Natural Sciences, Kyungpook National University, Taegu 702-701, South Korea

Received: December 17, 2007; In Final Form: February 5, 2008

The thermal decomposition mechanisms of chemisorbed methanol, ethanol, and 1-propanol on Si(100)-2 × 1 surface were theoretically investigated. Five different hydrogen elimination channels were found, which are one α-hydrogen elimination, two different β-hydrogen eliminations, and two different γ-hydrogen eliminations. They produce aldehyde, epoxide, alkene, oxetane, and cyclopropane as desorbing species, respectively. Among these, the α- and the β-hydrogen eliminations producing aldehyde and alkene are kinetically the most favorable. In addition, Si−O bond formation and molecular hydrogen desorption channels were also found to yield methane and molecular hydrogen as the final outcomes, respectively. On the basis of these results, new assignments for the previous experiments are suggested. Current theoretical study illustrates that thermal decompositions of adsorbed primary alcohol are the result of various competing reactions, and the particular position of hydrogen on alcohol plays a major role in the overall surface reactivity.

1. Introduction

The adsorption and chemical transformations of organic compounds on the silicon surface have been a subject of rigorous scientific investigation for several decades.[1] Interest in the chemisorption of organic molecules on semiconductor surfaces has been fueled by various present and potential applications. For example, the controlled deposition of organic films on surfaces has found applications in sensor technology, optoelectronic devices, nonlinear optical materials, and microelectronics.

The reactivity of these surfaces is strongly dependent on the electronic environment of surface atoms, which to a large extent is determined by the geometrical arrangement of atoms at the surface. The (100) surface of silicon, for example, undergoes a 2 × 1 reconstruction, resulting in the formation of rows of silicon surface dimers.[2] These dimers have been observed to undergo facile addition type reactions with active hydrogen compounds such as hydrogen halides,[3] alcohols,[4] and water,[5] as well as with amines[6] and phosphines.[7]

Raman spectroscopy,[4a] angle-resolved electron energy loss spectroscopy in reflection mode (REELS) experiments,[4b] Fourier transform reflection−absorption infrared spectroscopy (FT-RAIRS),[4c] and synchrotron radiation-excited photoemission and photon-stimulated desorption spectroscopies[4g] on the adsorption of methanol on Si(001) showed that it undergoes a dissociative adsorption forming $Si-OCH_3$ and Si−H species. The conclusion of facile O−H bond activation is also confirmed by Zhang et al.[8] using Auger electron spectroscopy (AES), low-energy diffraction (LEED), and thermal desorption spectroscopy (TDS) experiments.

Theoretically,[4d,e,8] it was shown that the molecular adsorption occurs barrierlessly via a stable chemisorbed state, and that there is a weak activation barrier for the dissociation process. These studies also pointed out that the C−O bond activation requires much higher activation energies. The preferential O−H bond activation was also confirmed by slab calculations.[9] Therefore, it is now a general consensus that the O−H bond cleavage of primary alcohol is the major channel producing surface alkoxy groups upon adsorption on the silicon (100)-2 × 1 surface.

On the other hand, their detailed nature of thermal decomposition mechanisms on the silicon surface is not clear in part because of the complexity of surface reactions. TDS study[8] on methanol, ethanol, and 1-propanol provided evidence for the hydrogen elimination channel of surface-bound alkoxy radicals, as well as for the competing surface decomposition channels. The major desorbing thermal decomposition for all of these species was reported to come from the β-hydrogen elimination of a surface-bound alkoxy radical to form an alkene, a reaction analogous to the formation of ethylene from surface-bound ethyl groups,[10] or imines from surface-bound amido radicals.[6i] In another thermal decomposition study of 1-pentanol and 2-methyl-1-butanol on the Si(100)-2 × 1 surface, the surface alkoxy species were reported to decompose via γ-hydrogen elimination mechanism to yield alkene at above 500 K.[11]

In this paper, the potential energy surfaces of thermal decompositions of chemisorbed methanol, ethanol, and 1-propanol on the Si(100)-2 × 1 surface were theoretically explored to obtain detailed decomposition mechanisms. We show that in addition to the β-, γ-hydrogen elimination channels, there exist various other possible competing channels.

2. Computational Details

To obtain the geometries and the energetics of adsorption and desorption reactions of primary alcohols, electronic structure calculations based on second-order Moller−Plesset perturbation theory (MP2) were performed using the cluster models of the Si(100)-2 × 1 surface. Since the initial reactant has a saturated surface dimer and the stationary points along the potential energy surfaces remain single configurational, the single reference methods would yield quantitatively reasonable results. All calculations reported here were performed with the general

* Author to whom correspondence should be addressed. Tel: +82-53-950-5332, Fax: +82-53-950-6330, e-mail: cchoi@knu.ac.kr.

10.1021/jp711840f CCC: $40.75
Published on Web 04/04/2008

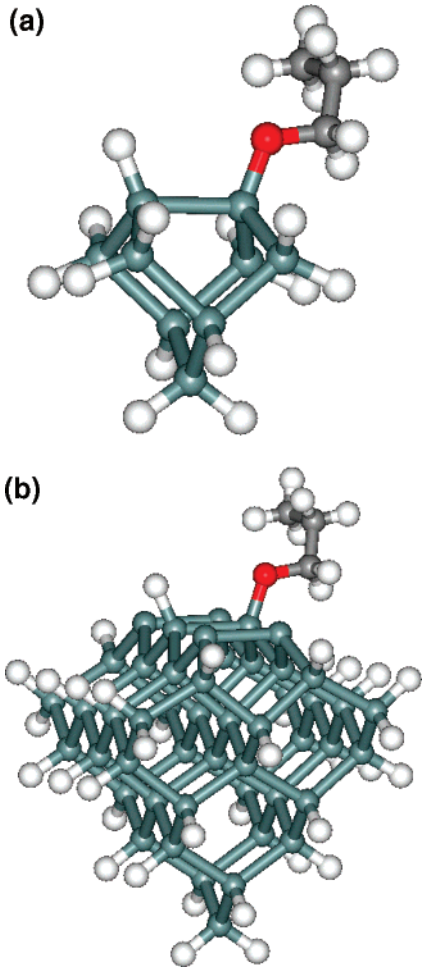

Figure 1. The illustrations of QM (a) and MM (b) regions of SIMOMM model used.

atomic and molecular electronic structure system (GAMESS).[12] The all-electron 6-31(d)[13] basis set was used throughout this work. The minimum energy reaction paths were determined by first optimizing the geometries of minima and transition states. The Hessian matrix (matrix of energy second derivatives) was computed and diagonalized for all stationery points to characterize them. In order to follow the minimum energy path (MEP), the Gonzalez−Schlegel second-order method[14] was used with a step size of 0.3 amu$^{1/2}$-bohr.

To study the surface size effects, a hybrid quantum mechanics/molecular mechanics (QM/MM) method called surface integrated molecular orbital molecular mechanics (SIMOMM)[15] was adopted, where the chemically inactive region of a system is calculated by the computationally inexpensive force field methods, while the chemically active part is treated by the quantum mechanics. It has been shown that the SIMOMM gives excellent results at relatively low computational cost.[16] In this work, the QM/MM models were designed such that $OCSi_9H_{16}$, $OC_2Si_9H_{18}$, and $OC_3Si_9H_{20}$ quantum regions are embedded in $OCSi_{48}H_{59}$, $OC_2Si_{48}H_{61}$, and $OC_3Si_{48}H_{63}$ clusters for the thermal decomposition studies of methanol, ethanol, and 1-propanol, respectively. These three models have one and three surface Si dimer(s) in the QM and MM regions, respectively. The illustrative figures of QM and MM regions are presented in Figure 1. MM3[17] parameters were used for the molecular mechanics part of computations. All computations were done without imposing symmetry unless otherwise specified.

3. Results and Discussions

As discussed in the introduction, primary alcohol on Si(100)-2 × 1 initially forms surface alkoxy groups via the O−H bond cleavage path. This is similar in nature to the predicted initial interaction of water[18] molecule with this surface. Since our current interest is to understand the thermal decomposition mechanisms of adsorbed primary alcohols, the initially adsorbed structure serves as a reference for other stationary points on the potential energy surface. 1-Propanol has α-, *β*-, *γ*-hydrogens with respect to its oxygen, while ethanol and methanol have α-, *β*-hydrogens and α-hydrogen, respectively. These hydrogens can interact with oxygen and surface silicon atoms yielding $H_\alpha-Si_b$, $H_\beta-Si_b$, $H_\beta-O$, $H_\gamma-Si_b$ and $H_\gamma-O$ interactions. Figure 2 represents the possible hydrogen elimination paths with their final outcomes. The energetic data are also summarized in Table 1. In the case of ethanol, there is no *γ*-hydrogen, so $H_\gamma-Si_b$ and $H_\gamma-O$ interactions are not possible. Likewise, only the $H_\alpha-Si_b$ interaction is available for methanol. In addition to the hydrogen involving reactions, other possible channels were studied, which shall be discussed in order.

A. $H_\alpha-Si_b$ Interaction. Aldehyde-Producing Channel. The α-2-Hydrogen can react with the surface Si, which is referred to as $H_\alpha-Si_b$ bond forming interaction. The fully optimized structures and relative energetics of stationary points along the $H_\alpha-Si_b$ reaction path as obtained with SIMOMM:MP2/6-31G* are shown in Figure 3. The transition state **TS1** connects the reference reactant **R1** with weakly bound intermediate **I1** with reaction barrier of 73.5 kcal/mol. The interaction of α-hydrogen and Si_b weakens the H_2-C_α and Si_b-O bonds. In the case of ethanol and methanol, the activation energies were calculated to be 74.4 and 78.7 kcal/mol, respectively. It can be seen that as the lengths of alky group increase, the barrier decreases, indicating that the electron-donating group reduces the reaction barrier. With small thermal energies, aldehyde molecule desorbs as shown in **P1**. The overall reactions of 1-propanol, ethanol, and methanol are endothermic by 28.2, 28.0, and 34.0 kcal/mol, respectively. Unlike experimentally suggested *β*-hydrogen elimination,[8] our theoretical results suggest the α-hydrogen elimination mechanism for the aldehyde desorption.

B. $H_\beta-Si_b$ Interaction. Epoxide-Producing Channel. In the case of ethanol and 1-propanol, *β*-hydrogen exists that can react with oxygen as well as with the surface silicon. In this channel, the *β*-4-hydrogen migrates from C_β to Si_b, producing the epoxide (see Figure 4). The transition state **TS2**, where H_4-Si_b and $O-C_\beta$ bonds are forming, connects the reactant (**R1** in Figure 3) with the intermediate **I2**. The reaction barriers of 1-propanol and ethanol are calculated to be 123.5 and 132.4 kcal/mol, respectively. These values are much higher than those of α-hydrogen elimination ($H_\alpha-Si_b$ interaction), which may be in part due to the highly strained three-membered ring in the transition state. The resulted epoixde is weakly bound to the surface hydrogens as shown in **I2**. The final product **P2** is endothermic by 55.6 kcal/mol. In the case of ethanol, it was calculated to be 57.0 kcal/mol. These values are also about 20 kcal/mol higher than those of aldehyde-producing channel. Therefore, the current epoxide-producing channel is both kinetically and thermodynamically much less favorable.

C. $H_\beta-O$ Interaction. Alkene-Producing Channel. In addition to the $H_\beta-Si_b$ bond forming interaction, the *β*-hydrogen can also interact with an oxygen atom, producing the alkene as shown in Figure 5. By forming the H_5-O and breaking $O-C_\alpha$ bonds, the transition state **TS3** connects the reactant **R1** with the physisorbed intermediate **I3**. The energy barriers of ethanol and 1-propanol were calculated to be 72.2 and 71.8 kcal/mol,

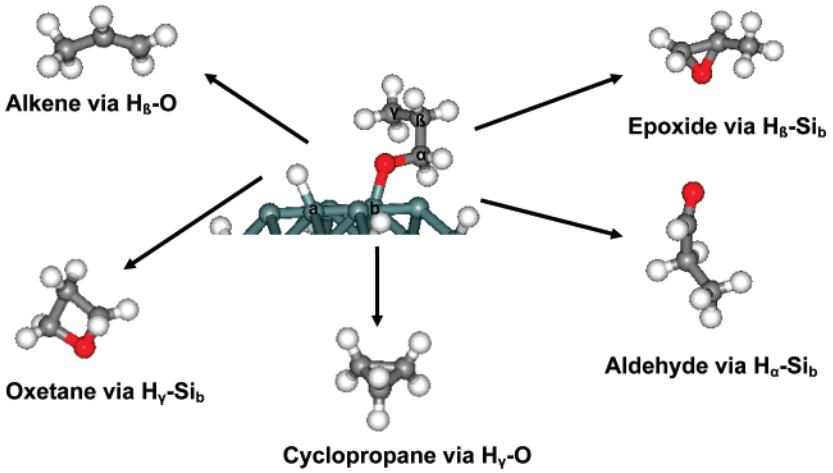

Figure 2. The illustrations of the hydrogen elimination reaction paths studied in this paper.

TABLE 1: The Overall Reaction Barriers, Energy Changes, and Desorption Products of Various Reaction Paths Studied in This Paper[a]

type	reaction barrier (methanol, **ethanol**, 1-*propanol*)	ΔH (methanol, **ethanol**, 1-*propanol*)	product
$H_\alpha-Si_b$	78.7, **74.4**, *73.5*	34.0, **34.2**, *34.7*	aldehyde
$H_\beta-Si_b$	**132.4**, *123.5*	**57.0**, *55.6*	epoxide
$H_\beta-O$	**72.2**, *71.8*	**20.5**, *17.2*	alkene
$H_\gamma-Si_b$	*121.2*	*60.9*	oxetane
$H_\gamma-O$	*95.4*	*28.0*	cyclopropane
$O-Si_a$	80.4	15.5	methane
H_2	88.9	38.6	H_2

[a] Energies are in kcal/mol. The numbers in normal, bold, and italic typefaces correspond to the energies of methanol, ethanol, and 1-propanol, respectively.

respectively. These values are slightly lower than those of the α-hydrogen elimination (the aldehyde-producing channel). With small thermal energies, alkene desorption occurs as shown in **P3**. The overall reactions of ethanol and 1-propanol are endothermic by 20.5 and 17.2 kcal/mol, respectively. These values are also smaller than those of α-hydrogen elimination. As a result, current alkene-producing channel via the *β*-hydrogen elimination is the most favorable path in the thermal desorptions of ethanol and 1-propanol. Unlike the experimental proposition of *γ*-hydrogen elimination mechanism,[11] it is suggested that the *β*-hydrogen elimination ($H_\beta-O$ in particular) is the main channel to produce alkene molecules.

D. $H_\gamma-Si_b$ Interaction. Oxetane-Producing Channel. In the case of 1-propanol, *γ*-hydrogen exists that can undergo hydrogen elimination reactions with surface silicon atom.(see Figure 6) By forming the Si_b-H_6 and $C_\gamma-O$ bonds simultaneously, the transition state **TS4** connects the reactant **R1** with the intermediate **I4**, with reaction barrier of 121.2 kcal/mol, which is much higher than those of aldehyde and alkene-producing channels. By breaking the weak hydrogen bonds shown in **I4**, the channel produces oxetane. The overall reaction is endothermic by 60.9 kcal/mol, making it thermodynamically the least favorable.

E. $H_\gamma-O$ Interaction. Cyclopropane-Producing Channel. The *γ*-hydrogen of 1-propanol can also interact with oxygen to produce cyclopropane.(see Figure 7). By forming H_7-O, the transition state **TS5** connects the reactant **R1** with the intermediate **I5,** with a reaction barrier of 95.4 kcal/mol. The overall reaction is endothermic by 28.0 kcal/mol. Consequently, current *γ*-hydrogen (H_7-O) elimination channel may not be as favorable as the aldehyde- and alkene-producing channels but is more favorable than the epoxide- and oxetane-producing channels. Therefore, in the case of 1-propanol, this channel can compete with the aldehyde- and alkene-producing channels depending on experimental conditions.

F. $O-Si_a$ Interaction. Methane-Producing Channel. In addition to the hydrogen elimination reactions, the oxygen of the surface methoxy group can react with the surface silicon of the dimer (see Figure 8). Nucleophilic attack of oxygen lone pair electrons initiates the reaction. The transition state **TS6** connects the reactant **R2** with the intermediate **I6**, with a reaction barrier of 65.7 kcal/mol. The surface Si_a-Si_b bond is broken and trivalent oxygen is formed in **I6**, which is 15.3 kcal/mol less stable than the reactant. By breaking the $O-C_\alpha$ and forming the $C_\alpha-H_1$ bonds, the second transition state **TS7** connects the **I6** with the weakly physisorbed intermediate **I7.** The reaction barrier of **TS7** is calculated to be 80.4 kcal/mol, which is slightly higher than that of $H_\alpha-Si_b$ reaction (aldehyde-producing channel). Methane is produced with the overall endothermicity of 15.5 kcal/mol, making it thermodynamically the most favorable. As a result, the current channel is as favorable as the aldehyde-producing channel. The same attempts to locate similar channels for ethoxy and propanoxy groups were not successful. In short, in the case of methanol decomposition, this current methane-producing channel can be one of the major reactions.

G. Desorption of Hydrogen Molecule. The alkene- the cyclopropane-producing channels (channels C and E) leave hydroxyl groups on the surface. These species may undergo subsequent hydrogen molecule desorption as shown in Figure 9. By forming the Si_a-O and H_1-H_2 bonds, the transition state **TS8** connects the reactant **R3** with the intermediate **I8**, with a reaction barrier of 88.9 kcal/mol. By breaking a weak hydrogen bond, the hydrogen molecule desorbs with the overall endothermicity of 38.6 kcal/mol. Compared to the other reactions, current hydrogen desorption channel is quite competitive both kinetically and thermodynamically.

H. General Considerations. The overall reaction barriers and enthalpies of reactions are summarized in Table 1. Among the hydrogen elimination channels, the $H_\beta-O$ and the $H_\alpha-Si_b$ channels are kinetically the most favorable, while the $H_\beta-Si_b$ and the $H_\gamma-Si_b$ channels are kinetically the least accessible. The $H_\gamma-O$ path is in between the two extremes. Consequently, it is expected that alkene and aldehyde, which are the outcomes of $H_\beta-O$ and $H_\alpha-Si_b$ channels, will be the major products of thermal decompositions. Epoxide and oxetane, which are the outcomes of $H_\beta-Si_b$ and $H_\gamma-Si_b$ channels, are expected to be the minor products. In the case of 1-propanol, the cyclopropane

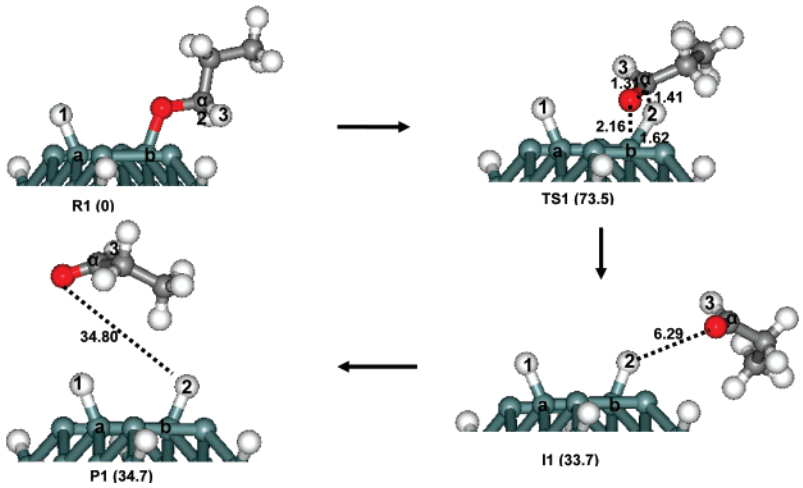

Figure 3. The geometric data and relative energies along the aldehyde-producing channel via $H_\alpha-Si_b$ interaction. Bond lengths and energies are in angstroms and kcal/mol.

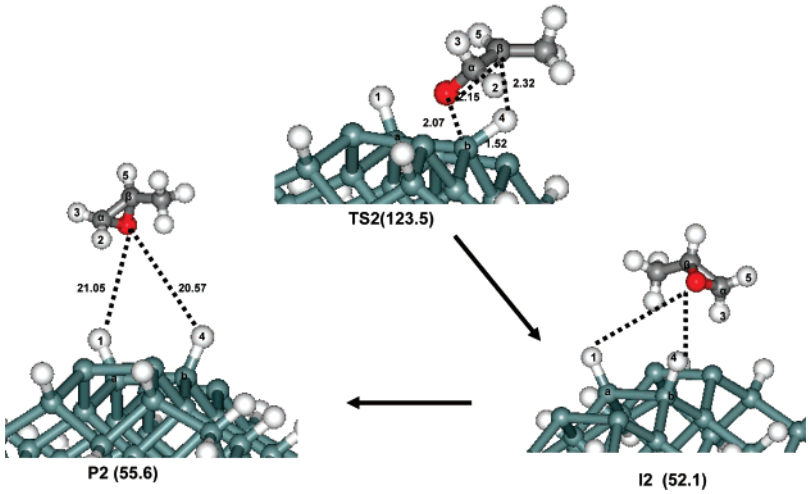

Figure 4. The geometric data and relative energies along the epoxide-producing channel the via $H_\beta-Si_b$ interaction. Bond lengths and energies are in angstroms and kcal/mol.

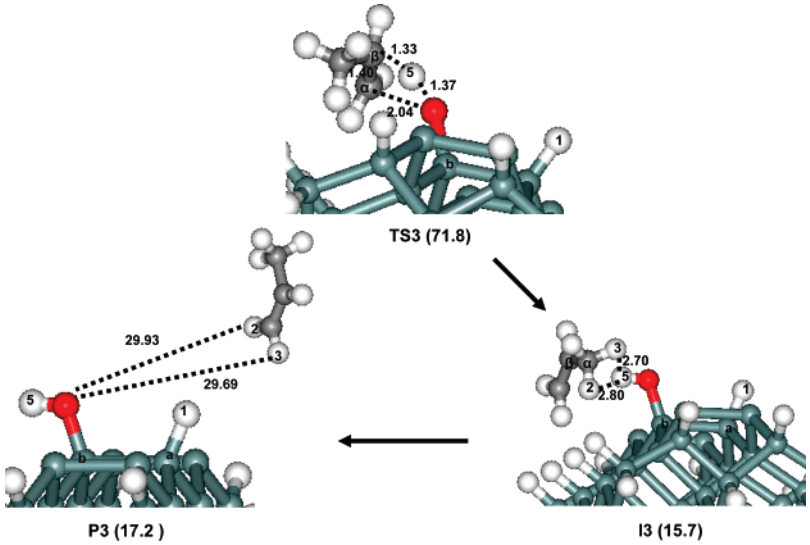

Figure 5. The geometric data and relative energies along the alkene-producing channel via $H_\beta-O$ interaction. Bond lengths and energies are in angstroms and kcal/mol.

desorption of $H_\gamma-O$ channel can be important. In addition to the hydrogen elimination channels, the $O-Si_a$ and the H_2 channels are good reaction competitors. Zhang et al.[8] have reported that thermal desorption peaks observed after room-temperature adsorption of 1-propanol on Si(100) occur at *m/e* = 58, 44, 42, 26, and 2. The first *m/e* = 58 has the peak desorption temperature of 670 K. According to our calculations, the possible candidates are propanal, 3-methyloxirane, and

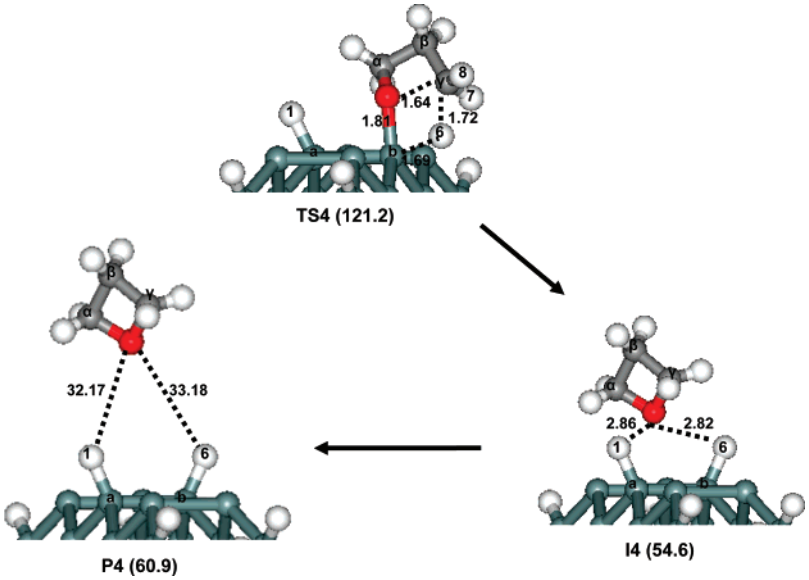

Figure 6. The geometric data and relative energies along the oxetane-producing channel via $H_\gamma-Si_b$ interaction. Bond lengths and energies are in angstroms and kcal/mol.

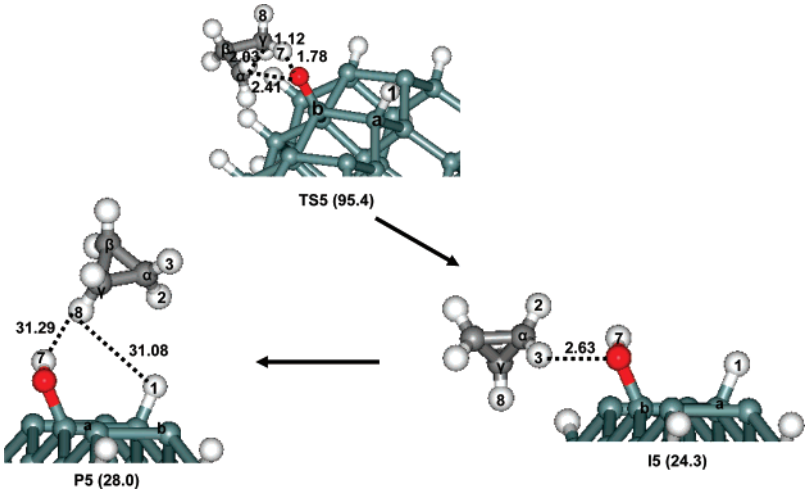

Figure 7. The geometric data and relative energies along the cyclopropane-producing channel via $H_\gamma-O$ interaction. Bond lengths and energies are in angstroms and kcal/mol.

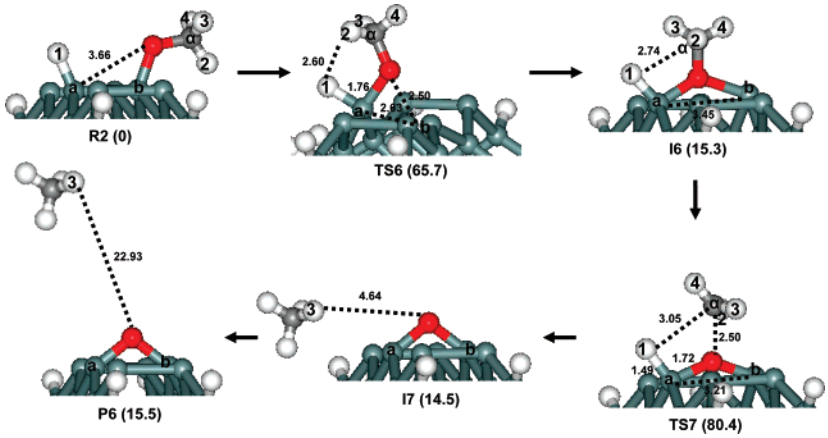

Figure 8. The geometric data and relative energies along the methane formation channel via $O-Si_a$ interaction. Bond lengths and energies are in angstroms and kcal/mol.

oxetane. However, the reaction barrier of propanal is much lower than the other two species. Therefore, the peak at $m/e = 58$ can be safely assigned as propanal molecule, which is consistent with the experimental assignment. Experimentally the β-hydrogen elimination was suggested as a possible mechanism. However, our calculation revealed that the propanal desorption is due to the α-hydrogen elimination. The peaks at $m/e = 44$ was experimentally assigned as SiO desorption. No relevant thermal decomposition of primary alcohol channel is found in our calculations, which may support the experimental assign-

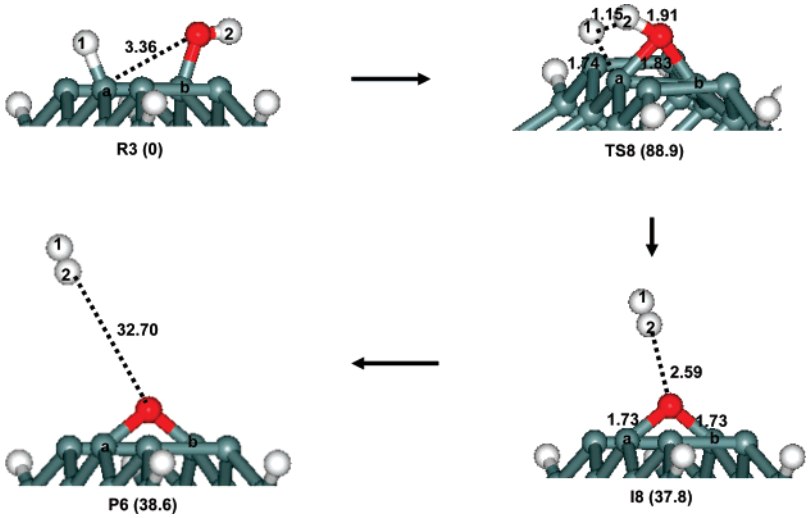

Figure 9. The geometric data and relative energies along the hydrogen desorption channel. Bond lengths and energies are in angstroms and kcal/mol.

ment. The *m/e* = 42 species displays two peaks at 485 and 670 K, which were experimentally assigned as propylene and ionization-induced cracking of the *m/e* = 58 peak, respectively. According to our calculations, the two peaks can be assigned as propylene and cyclopropane desorptions, respectively, since both reactions have relatively low reaction barriers. Our calculations show that they are results of β- and γ-hydrogen eliminations, respectively. The *m/e* = 26 species was assigned as ionization-induced cracking fragments. Our calculations also did not provide the possibility of thermal decomposition. The *m/e* = 2 species of peak at 825 K was experimentally assigned as molecular hydrogen, whose mechanism is provided by our calculations in section G.

The thermal desorption of ethanol also revealed four major desorption products having *m/e* = 44, 28, 26, and 2.[8] The *m/e* = 44 products have peaks at 630 and 960 K, which were experimentally assigned as acetaldehyde and SiO desorption. The acetaldehyde assignment is confirmed by our calculations. Another candidate for this peak would be epoxide according to our calculations, although its possibility would be low. The products *m/e* = 28 and 26 were experimentally explained as ionization-induced cracking. However, ethylene desorption can be an excellent candidate for the *m/e* = 28 species. As in the case of 1-propanol, the *m/e* = 2 can be assigned as molecular hydrogen.

The thermal decompositions of methanol also revealed desorption products having the *m/e* = 44, 30, 28, 16, and 2.[8] As in the case of above results, the *m/e* = 44, 28, and 2 were experimentally assigned as SiO desorption, cracking product, and molecular hydrogen, respectively. The *m/e* = 30 species was experimentally assigned as formaldehyde, which is confirmed by our calculations. Experimentally, the *m/e* = 16 species was not clearly assigned, which can be assigned as methane desorption via the O−Si_a channel.

4. Conclusions

The thermal decompositions of methanol, ethanol, and 1-propanol adsorbed on the Si(100)-2 × 1 surface were theoretically investigated. The O−H cleaved structure served as the reference stationary point of subsequent surface reactions. We found seven thermal decomposition channels. Five of them are hydrogen elimination channels. The α-hydrogen elimination channel is initiated by the formation of the H_α−Si bond, which eventually leads to the aldehyde desorption. Two different β-hydrogen elimination channels were found. They are classified as the H_β−Si and the H_β−O paths, which lead to epoxide and alkene, respectively. Just like the β-hydrogen eliminations, the two different γ-hydrogen eliminations of 1-propanol are possible depending on the reacting atom (H_γ−Si and H_γ−O). These two γ-hydrogen eliminations produce oxetane and cyclopropane, respectively. In addition to these hydrogen eliminations, the Si−O and molecular hydrogen paths were also found leading to methane and molecular hydrogen desorptions, respectively.

The calculated overall reaction barriers indicate that the aldehyde (H_α−Si)- and the alkene (H_β−O)-producing channels are kinetically the most favorable, followed by the cyclopropane channel of 1-propanol and the methane channel of methanol. Previous experiments suggested that the aldehyde- and the alkene-producing channels were due to β- and γ-hydrogen eliminations. However, according to our theoretical calculations, they are due to α- and β-hydrogen eliminations. The α-hydrogen of alcohol can be regarded as β-hydrogen with respect to the surface Si. Therefore, the two most facile α- and β-hydrogen eliminations can be considered as the β-hydrogen effect. On the basis of our mechanisitic results, previous experiments were reinterpreted.

Current theoretical study illustrates that the thermal decompositions of adsorbed alcohol are composed of various reactions, and the particular position of hydrogen on alcohol plays a major role in the overall surface reactivity.

Acknowledgment. This work was supported by the Korea Science and Engineering Foundation (KOSEF) Grant funded by the Korean Government (MOST) (R11-2007-012-03001-0).

References and Notes

(1) Waltenburg, H. N.; Yates, J. T., Jr. *Chem. Rev.* **1995**, *95*, 1589−1673.

(2) (a) Chadi, D. J. *Phys. Rev. Lett.* **1979**, *43*, 43−47. (b) Hamers, R. J.; Tromp, R. M.; Demuth, J. E. *Phys. Rev. B* **1986**, *34*, 5343−5357. (c) Boland, J. J. *Adv. Phys.* **1993**, *42*, 129−171. (d) Duke, C. B. *Chem. Rev.* **1996**, *96*, 1237−1259. (e) Hata, K.; Yasuda, S.; Shigekawa, H. *Phys. Rev. B* **1999**, *60*, 8164−8170.

(3) (a) Johnson, A. L.; Walczak, M. M.; Madey, T. E. *Langmuir* **1988**, *4*, 277−282. (b) Craig, B. I.; Smith, O. V. *Surf. Sci.* **1992**, *262*, 235−244. (c) Gao, Q.; Cheng, C. C.; Chen, P. J.; Choyke, W. J.; Yates, J. T. *Thin Solid Films* **1993**, *225*, 140−144.

(4) (a) C. Shannon, A. Campion, *Surf. Sci.* **1990**, *227*, 219. (b) Ch. Kleint, S. M. A. *El Halim, Surf. Sci.* **1991**, *247*, 375. (c) Ehrley, W.; Butz, R.; Mantl, S. *Surf. Sci.* **1991**, *248*, 193−200. (d) Lu, X.; Zhang, Q.; Lin,

M. C. *Phys. Chem. Chem. Phys.* **2001**, *3*, 2156−2161. (e) Kato, T.; Kang, S.-Y.; Xu, X.; Yamabe, T. *J. Phys. Chem. B* **2001**, *105*, 10340−10347. (f) Casaletto, M. P.; Zanoni, R.; Carbone, M.; Piancastelli, M. N.; Aballe, L.; Weiss, K.; Horn, K. *Surf. Sci.* **2002**, *505*, 251−259. (g) Eng, J.; Raghavachari, K.; Struck, L. M.; Chabal, Y. J.; Bent, B. E.; Flynn, G. W.; Christman, S. B.; Chaban, E. E.; Williams, G. P.; Radermacher, K.; Mantl, S. *J. Chem. Phys.* **1997**, *106*, 9889−9898. (h) Casaletto, M. P.; Zanoni, R.; Carbone, M.; Piancastelli, M. N.; Aballe, L.; Weiss, K.; Horn, K. *Surf. Sci.* **2000**, *447*, 237−244.

(5) (a) Chabal, Y. J. *Surf. Sci. Rep.* **1988**, *8*, 211−357. (b) Konecny, R.; Doren, D. J. *J. Chem. Phys.* **1997**, *106*, 2426−2435. (c) Niwano, M.; Terashi, M.; Shinohara, M.; Shoji, D.; Miyamoto, N. *Surf. Sci.* **1998**, *401*, 364−370. (d) Weldon, M. K.; Queeney, K. T.; Gurevich, A. B.; Stefanov, B. B.; Chabal, Y. J.; Raghavachari, K. *J. Chem. Phys.* **2000**, *113*, 2440−2446.

(6) (a) Dresser, M. J.; Taylor, P. A.; Wallace, R. M.; Choyke, W. J.; Yates, J. T. *Surf. Sci.* **1989**, *218*, 75−107. (b) Fujisawa, M.; Taguchi, Y.; Kuwahara, Y.; Onchi, M.; Nishijima, M. *Phys. Rev. B* **1989**, *39*, 12918−12920. (c) Larsson, C. U. S.; Flodstrom, A. S. *Surf. Sci.* **1991**, *241*, 353−356. (d) Franco, N.; Avila, J.; Davila, M. E.; Asensio, M. C.; Woodruff, D. P.; Schaff, O. V.; Fernandez, V.; Schindler, K.-M.; Bradshaw, A. M. *J. Phys.: Condens. Matter* **1997**, *9*, 8419−8432. (e) Widjaja, Y.; Mysinger, M. M.; Musgrave, C. B. *J. Phys. Chem. B* **2000**, *104*, 2527−2533. (f) Mulcahy, C. P. A.; Carman, A. J.; Casey, S. M. *Surf. Sci.* **2000**, *459*, 1−13. (g) Mui, C.; Wang, G. T.; Bent, S. F.; Musgrave, C. B. *J. Chem. Phys.* **2001**, *114*, 10170−10180. (h) Cao, X.; Hamers, R. J. *J. Am. Chem. Soc.* **2001**, *123*, 10988−10996. (i) Carman, A. J.; Zhang, L.; Liswood, J. L.; Casey, S. M. *J. Phys. Chem. B* **2003**, *107*, 5491−5502.

(7) (a) Colaianni, M. L.; Chen, P. J.; Yates, J. T. *J. Vac. Sci. Technol. A* **1994**, *12*, 2995−2998. (b) Shan, J.; Wang, Y.; Hamers, R. J. *J. Phys. Chem.* **1996**, *100*, 4961−4969. (c) Miotto, R.; Srivastava, G. P.; Miwa, R. H.; Ferraz, A. C. *J. Chem. Phys.* **2001**, *114*, 9549−9556.

(8) Zhang, L.; Carman, A. J.; Casey, S. M. *J. Phys. Chem. B* **2003**, *107*, 8424.

(9) (a) Silvestrelli, P. L. *Surf. Sci.* **2004**, *552*, 17. (b) Miotto, R.; Srivastava, G. P.; Ferraz, A. C. *Surf. Sci.* **2005**, *575*, 287.

(10) (a) Keeling, L. A.; Chen, L.; Greenlief, C. M.; Mahajan, A.; Bonser, D. *Chem. Phys. Lett.* **1994**, *217*, 136−141. (b) Darlington, B.; Foster, M.; Campion, A. *Surf. Sci.* **1994**, *304*, L407−L412. (c) Du, W.; Keeling, L. A.; Greenlief, C. M. *J. Vac. Sci. Technol. A* **1994**, *12*, 2281−2286. (d) Klug, D.-A.; Greenlief, C. M. *J. Vac. Sci. Technol. A* **1996**, *14*, 1826−1831. (e) Foster, M.; Darlington, B.; Scharff, J.; Campion, A. *Surf. Sci.* **1997**, *375*, 35−44. (f) Sampson, G. A.; White, J. M.; Ekerdt, J. G. *Surf. Sci.* **1998**, *411*, 163−175. (g) Bulanin, K. M.; Shah, A. G.; Teplyakov, A. V. *J. Chem. Phys.* **2001**, *115*, 7187−7195.

(11) Yoon, W. J.; Lee, J. P.; Park, G.; Park, C. R.; Kwak, H. T.; Sung, M. M. *J. Vaccum Sci., Technol. A* **2003**, *21*, 740.

(12) (a) Schmidt, M. W.; Baldridge, K. K.; Boatz, J. A.; Elbert, S. T.; Gordon, M. S.; Jensen, J. H.; Koseki, S.; Matsunaga, N.; Nguyen, K. A.; Su, S.; Windus, T. L.; Dupuis, M.; Montgomery, J. A., Jr. *J. Comput. Chem.* **1993**, *14*, 1347. (b) Fletcher, G. D.; Schmidt, M. W.; Gordon, M. S. *Adv. Chem. Phys.* **1999**, *110*, 267.

(13) Hehre, W. J.; Ditchfield, R.; Pople, J. A. *J. Chem. Phys.* **1972**, *56*, 2257.

(14)) (a) Gonzalez, C.; Schlegel, H. B. *J. Phys. Chem.* **1990**, *94*, 5523. (b) Gonzalez, C.; Schlegel, H. B. *J. Chem. Phys*. **1991**, *95*, 5853.

(15) Shoemaker, J. R.; Burgraff, L. W.; Gordon, M. S. *J. Phys. Chem. A* **1999**, *103*, 3245.

(16) (a) Choi, C. H.; Gordon, M. S. *J. Am. Chem. Soc.* **1999**, *121*, 11311. (b) Choi, C. H.; Gordon, M. S. *The Chemistry of Organic Silicon Compounds*; Rappoport, Z., Apeloig, Y., Eds.; John Wiley & Sons: New York, 2001; Vol. 3, Chapter 15, pp 821−852. (c) Choi, C. H.; Gordon, M. S. Theoretical Studies of Silicon Surface Reactions with Main Group Absorbates. In *Computational Materials Chemistry: Methods and Applications*; Curtiss, L. A., Gordon, M. S., Eds.; Kluwer Academic Publishers: Boston, 2004; Chapter 4, pp 125−190.

(17) (a) Allinger, N. L.; Yuh, Y. H.; Lii, J. H. *J. Am. Chem. Soc*. **1989**, *111*, 8551. (b) Lii, J. H.; Allinger, N. L. *J. Am. Chem. Soc.* **1989**, *111*, 8566. (c) Lii, J. H.; Allinger, N. L. *J. Am. Chem. Soc*. **1989**, *111*, 8576.

(18) Lee, H. S.; An, K.; Kim, Y.; Choi, C. H. *J. Phys. Chem. B* **2005**, *109*, 10909.